

## Supporting Information

### **Compartmentalization in Hybrid Metallocarborane Nanoparticles Formed by Block Copolymers with Star-Like Architecture**

Vladimír Ďord'ovič, Mariusz Uchman,<sup>\*</sup> Alexander Zhigunov, Antti Nykänen, Janne Ruokolainen, Pavel Matějček<sup>\*</sup>

<sup>\*</sup> Department of Physical and Macromolecular Chemistry, Faculty of Science, Charles University, Hlavova 2030, 128 40 Prague 2, Czech Republic.

pavel.matejcek@natur.cuni.cz, mariuszuchman@go2.pl

## Experimental Section

### Materials

Cesium salt of metallacarborane anion [3-cobalt(III) bis(1,2-dicarbollide)](-1), Cs[CoD], was purchased from Katchem Ltd. (Czech Republic) and it was converted to Na[CoD].4H<sub>2</sub>O by an extraction method described by Plešek.<sup>1</sup>

The poly(2-ethyl oxazoline) linear homopolymer, PEOX, was purchased from Aldrich with the weight averaged relative molecular weight  $5 \times 10^4$ . The linear poly(ethylene oxide), PEO, was purchased from Fluka with the weight averaged relative molecular weight  $41.5 \times 10^3$  and  $\bar{D} = 1.10$ .

The homo-arm star double-hydrophilic diblock copolymer [poly(ethylene oxide)-*block*-poly(2-methyl oxazoline)]<sub>4</sub>, [PEO-PMOX]<sub>4</sub>, linear double-hydrophilic diblock copolymers poly(ethylene oxide)-*block*-poly(2-ethyl oxazoline), PEO-PEOX and PEO-PEOX(2), and linear double-hydrophilic triblock copolymer poly(2-ethyl oxazoline)-*block*-poly(ethylene oxide)-*block*-poly(2-ethyl oxazoline), PEOX-PEO-PEOX, were purchased from Polymer source, Inc. (Dorval, Quebec, Canada). Only results of [PEO-PMOX]<sub>4</sub> and PEO-PEOX samples (structures in Scheme 1) are described in the main text, while data on other two samples are shown in Supporting Information only. As provided by Polymer Source, all the block copolymers have been prepared from PEO pre-polymers (mPEO for diblocks, PEO for triblock, and PEO star with pentaerythritol core for 4-arm star) with desired molar mass and low dispersity by additional polymerization of POX blocks.

**Table S1:** Characterization of block copolymers based on <sup>1</sup>H NMR and GPC measurements.

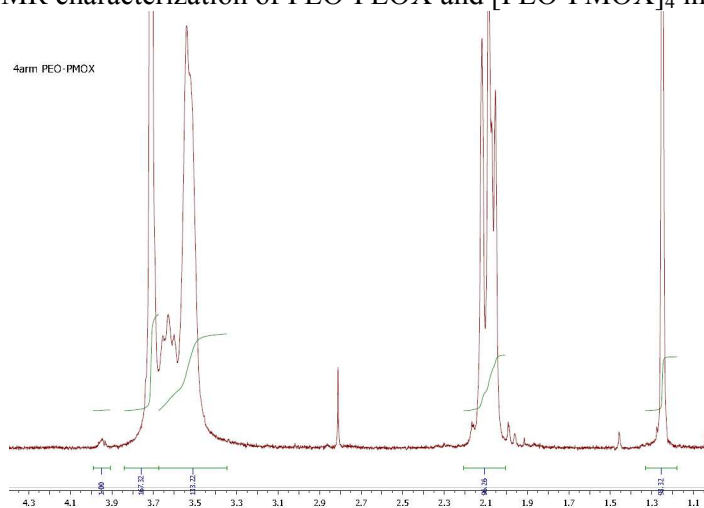
Sample	$M_n(\text{PEO})$ , NMR	$M_n(\text{POX})$ , NMR	$w(\text{PEO})$ , NMR	$\bar{D}$ , GPC
PEO-PEOX	4100	5100	0.45	1.8
[PEO-PMOX] <sub>4</sub>	4 × 3700	4 × 5600	0.40	1.5
PEO-PEOX(2)	5600	7000	0.44	1.8
PEOX-PEO-PEOX	4500	2 × 5000	0.31	1.6

We characterized all the block copolymers PEO-PEOX, PEO-PEOX(2), PEOX-PEOPEOX and [PEO-PMOX]<sub>4</sub> by standard GPC and NMR measurements, and the results are summarized in Table 1.  $M_n$  of all blocks were calculated by comparing of PEO and POX signals with the terminal group signals as shown in NMR spectra for PEO-PEOX and [PEO-PMOX]<sub>4</sub> below (Figure S1). GPC measurements were used for determination of dispersity ( $\bar{D}$ ) of block copolymers; all the chromatograms were monomodal. While PEO-PEOX, PEO-

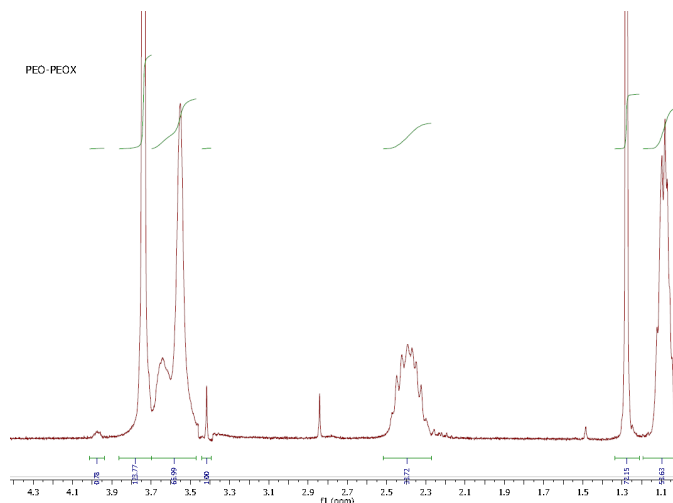
PEOX(2) and PEOX-PEOX samples are of a linear architecture, [PEO-PMOX]<sub>4</sub> macromolecule has a star-like shape with the pentaerythritol “core” and with four PMOX block on the periphery. Lengths of PEO and POX blocks in all the studied samples are comparable, and PEO blocks are always a bit longer; (PEO in the range 84 – 128 segments, and POX in the range 51 – 71 segments). The overall dispersities of block copolymers are fairly high (1.5 – 1.8), and it is given mainly by POX blocks, since PEO prepolymers had dispersities only around 1.1.

**Figure S1:**

<sup>1</sup>H NMR characterization of PEO-PEOX and [PEO-PMOX]<sub>4</sub> in water



Signal assignment for [PEO-PMOX]<sub>4</sub>: HO-CH<sub>2</sub>CH<sub>2</sub>-N (end group) 3.95; O-CH<sub>2</sub>CH<sub>2</sub> 3.7; N-CH<sub>2</sub>CH<sub>2</sub> 3.65-3.4; NCO-CH<sub>3</sub> 2.1; internal standard t-BuOH 1.25.



Signal assignment for PEO-PEOX: HO-CH<sub>2</sub>CH<sub>2</sub>-N (terminal group) 3.95; O-CH<sub>2</sub>CH<sub>2</sub> 3.7; N-CH<sub>2</sub>CH<sub>2</sub> 3.65-3.4; CH<sub>3</sub>-O (terminal group) 3.4; NCO-CH<sub>2</sub>CH<sub>3</sub> 2.4; internal standard t-BuOH 1.25; NCO-CH<sub>2</sub>CH<sub>3</sub> 1.1.

### ***Sample preparation***

The light scattering (LS) titration experiments for monitoring of the nanoparticle formation were carried out as follows: Stock aqueous solution of Na[CoD] (0.0245 M) was consecutively added to PEO-PEOX or [PEO-PMOX]<sub>4</sub> solutions (2 g/L, 5 mL) in 0.154 M NaCl. The solutions during the titration process were analyzed by a measuring of light scattering.

The samples for SAXS/SANS study were prepared by quick addition of Na[CoD] solution in 0.154 M NaCl to 200  $\mu$ L of relatively concentrated PEO-PEOX solution (10 g/L) in 0.154 M NaCl.

The samples for NMR study were prepared by mixing of calculated amount of solid Na[CoD] with 1 mL of PEO-PEOX solution (10 g/L) in 0.154 M NaCl in D<sub>2</sub>O in order to obtain mixtures with [CoD]-to-polymer segment ratio  $\xi = 0.015, 0.045$  and  $0.150$ . Small amount (1  $\mu$ L) of *t*-butyl alcohol (*t*-BuOH) was added to the solutions as an internal standard.

### ***Methods***

*Dynamic Light Scattering (DLS) and Static Light Scattering (SLS).* The light scattering setup (ALV, Langen, Germany) consisted of a 633 nm He-Ne laser, an ALV CGS/8F goniometer, an ALV High QE APD detector, and an ALV 5000/EPP multibit, multitaup autocorrelator. DLS data analysis was performed by fitting the measured normalized intensity autocorrelation function  $g_2(t) = 1 + \beta|g_1(t)|^2$ , where  $g_1(t)$  is the electric field correlation function,  $t$  is the lag-time and  $\beta$  is a factor accounting for deviation from the ideal correlation. An inverse Laplace transform of  $g_1(t)$  with the aid of a constrained regularization algorithm (CONTIN) provides the distribution of relaxation times,  $\tau A(\tau)$ . Effective angle- and concentration-dependent hydrodynamic radii,  $R_H(q,c)$ , were obtained from the mean values of relaxation times,  $\tau_m(q,c)$ , of individual diffusive modes using the Stokes-Einstein equation. To obtain true hydrodynamic radii, the data have to be extrapolated to a zero scattering angle.

*Electrophoretic light scattering.* The measurements were carried out with a Nano-ZS Zetasizer (Malvern Instruments, UK). Zeta-potential values were calculated from electrophoretic mobilities (averages of 15 to 100 measurements) using the Smoluchowski approximation.

*Atomic force microscopy (AFM).* AFM measurements were performed in the semicontact (tapping) mode under ambient conditions using a scanning probe microscope Digital Instruments NanoScope dimensions 3 equipped with a Nanosensors silicon cantilever. The nanoparticles were deposited from very dilute solutions (ca. 0.01 g/L) on a freshly cleaved mica surface. The samples were left to dry in a vacuum oven.

*Cryo-Transmission electron microscopy (cryo-TEM).* Cryo-TEM was carried out using field emission cryo-electron microscope (JEOL JEM-3200FSC), which was operating at 300 kV voltage. Images were taken in bright field mode and using zero loss energy filtering (omega type) with the slit width of 20 eV. Micrographs were recorded using Gatan Ultrascan 4000 CCD camera. Specimen temperature was maintained at  $-187\text{ }^{\circ}\text{C}$  during the imaging. Vitrified specimens were prepared using automated FEI Vitrobot device using Quantifoil 3.5/1 holey carbon copper grids with the hole size of  $3.5\text{ }\mu\text{m}$ . Just prior to use grids were plasma cleaned by Gatan Solarus 9500 plasma cleaner and then transferred into an environmental chamber of FEI Vitrobot having room temperature and 100 % humidity. Thereafter  $3\text{ }\mu\text{l}$  of sample solution was applied on the grid and it was blotted once for 1 seconds and then vitrified in 1/1 mixture of liquid ethane and propane at temperature of  $-180\text{ }^{\circ}\text{C}$ . The grid with vitrified sample solution were maintained at liquid nitrogen temperature and then cryo transferred in to the microscope.

*Small Angle X-ray Scattering (SAXS).* SAXS experiments were performed using a pinhole camera (Molecular Metrology SAXS System) attached to a microfocussed X-ray beam generator (Osmic MicroMax 002) operating at 45 kV and 0.66 mA (30 W). The camera was equipped with a multiwire gas-filled area, detector with an active area diameter of 20 cm (Gabriel design). Two experimental setups were used to cover the  $q$  range of  $0.005 - 1.1\text{ }\text{\AA}^{-1}$ . Scattering vector,  $q$ , is defined as:  $q = (4\pi/\lambda)\sin\theta$ , where  $\lambda$  is the wavelength and  $2\theta$  is the scattering angle. The scattering intensities were put on absolute scale using a glassy carbon standard.

*Small Angle Neutron Scattering (SANS).* SANS experiments were performed with the two-detector system<sup>2</sup> at the YuMO instrument (Dubna, Russia). The covered  $q$  range was  $0.07 - 0.2\text{ }\text{\AA}^{-1}$ . The solution was placed into Hellma standard cells with the thickness of 1 mm in the direction of neutron beam. The experimental data were treated with SAS package.<sup>3</sup>

*<sup>1</sup>H NMR spectroscopy.* <sup>1</sup>H NMR spectra were measured on a Varian <sup>UNITY</sup>INOVA 300 in deuterium oxide (99.5 %; Chemotrade, Leipzig, Germany). Spectra were referenced to the solvent signal (4.80 ppm).

*Isothermal Titration Calorimetry (ITC).* ITC measurements were performed with an Isothermal Titration Calorimeter (Nano ITC), TA Instruments – Waters LLC, (New Castle, USA). The microcalorimeter consists of a reference cell and a sample cell (24K Gold). The sample cell is connected to a 50  $\mu\text{L}$  syringe. The syringe needle is equipped with a flattened, twisted paddle at the tip, which ensures continuous mixing of the solutions in the cell rotating at 250 rpm. Titrations were carried out by consecutive 2  $\mu\text{L}$  injections of 6.125 mM Na[CoD] in 0.154 M NaCl aqueous solutions from the syringe into the sample cell filled with 193  $\mu\text{L}$  of 0.35 g/L [PEO-PMOX]<sub>4</sub> and 0.37 g/L PEO-PEOX in 0.154 M NaCl aqueous solution, and pure 0.154 M NaCl. By this method then the differential heat of mixing is determined for discrete changes of composition. The raw heat changes were analyzed by NITPIC software in order to obtain ITC thermograms. We carefully tuned experimental conditions to reach the minimum of noise prior the measurements.

## Interaction of PEO and PEOX homopolymers with NaCoD

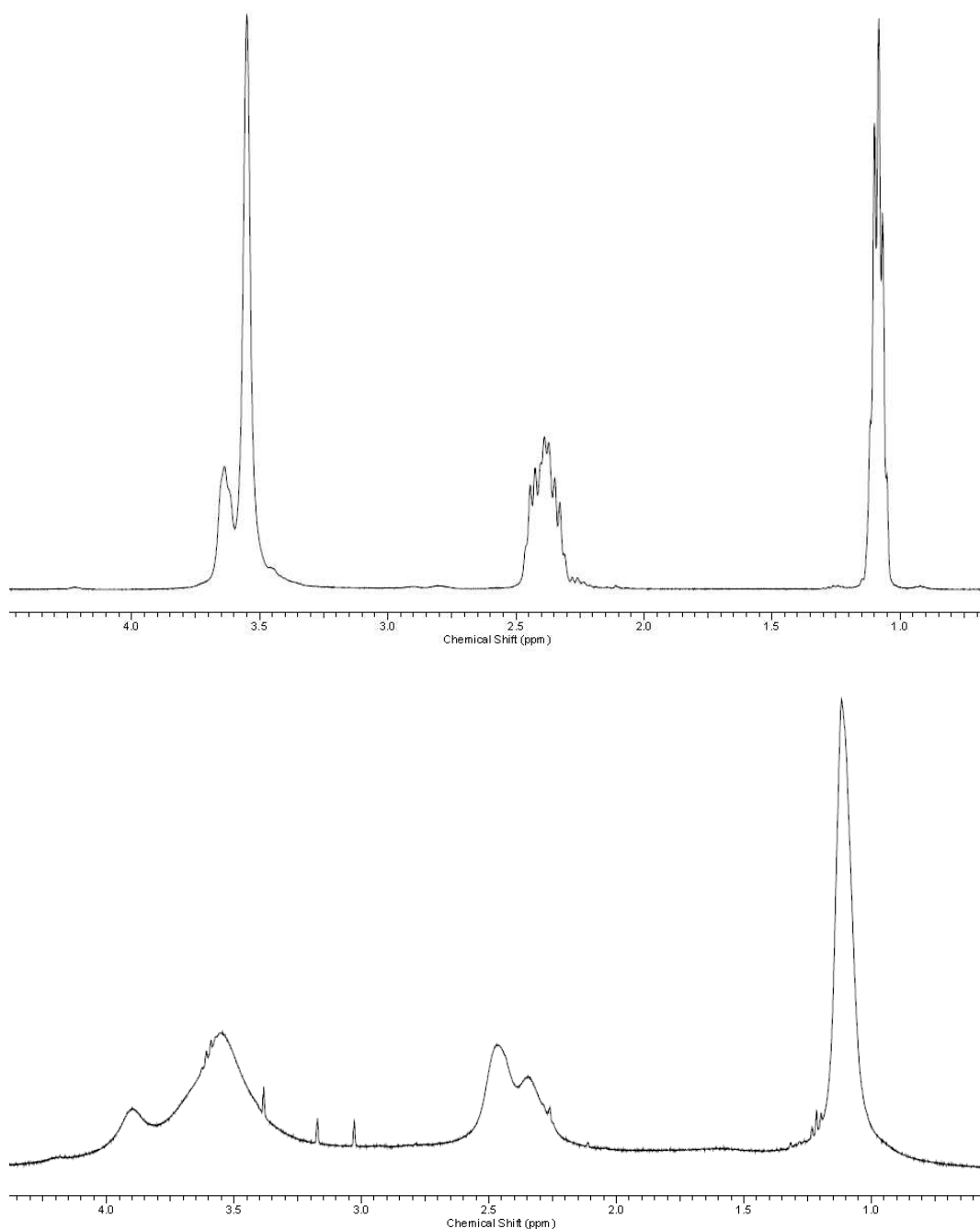
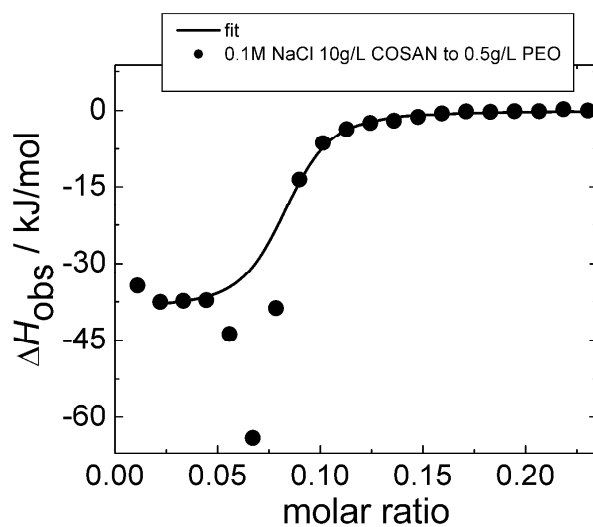
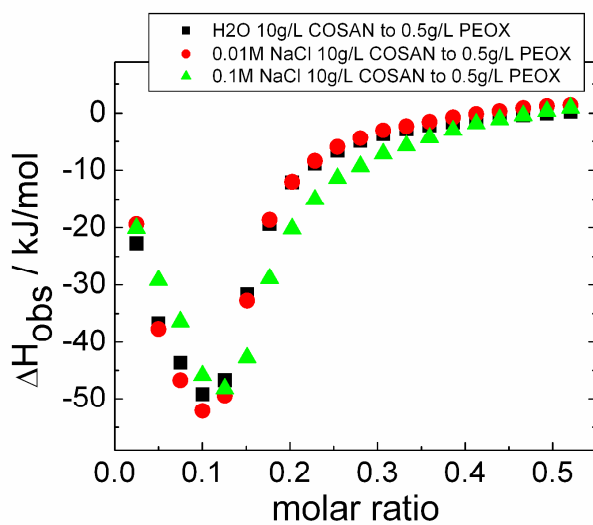


**Figure S2** Comparison of <sup>1</sup>H NMR spectra of (top) PEOX homopolymer and (bottom) its metallacarborane complex PEOX/Na[CoD] ( $\xi = 0.11$ ) in heavy water (ethylene backbone around 3.5 ppm; ethyl side group around 2.5 and 1 ppm). Interaction with metallacarborane leads to distinct broadening mainly of ethylene signals of the backbone.



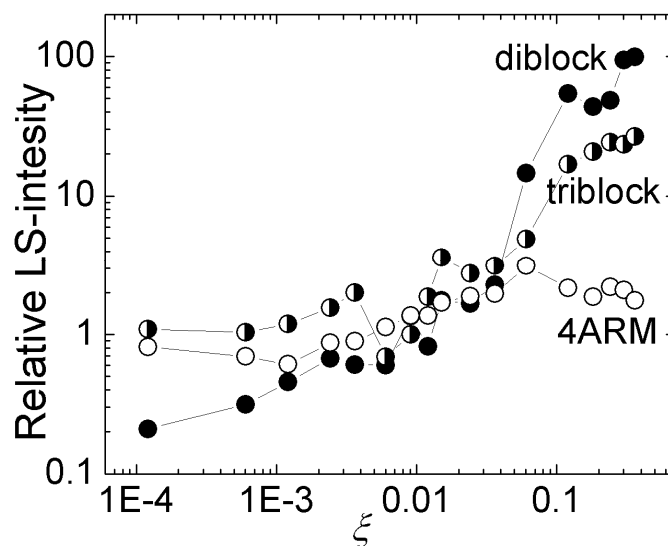
A



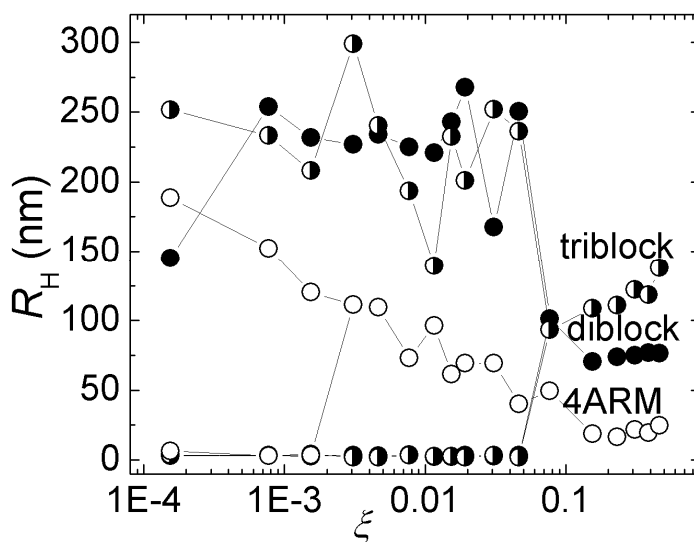
B

**Figure S3** ITC thermograms of (A) PEO homopolymer in water and (B) PEOX homopolymer in water and NaCl solutions during titration by Na[CoD] solution. In both cases, the complex formation is strongly exothermic with comparable interaction heats. In the case of PEO, strongly exothermic “aggregation” peak related to formation of highly organized insoluble nanocomposite is observed.

## Additional SLS&DLS characterization of nanoparticles



A



B

**Figure S4** Dependence of (A) relative light scattering intensity and (B) hydrodynamic radius,  $R_H$ , on the addition of  $\text{Na}[\text{CoD}]$  to (diblock) PEO-PEOX, (triblock) PEOX-PEO-PEOX, and (4ARM)  $[\text{PEO-PMOX}]_4$  solutions (2 g/L) in 0.154 M NaCl. It is evident that size and formation of nanoparticles formed by triblock copolymer are very similar to those of diblock copolymer, which confirms our assumption that linear architecture of block copolymers leads to similar type of nanoparticles. In both cases, we observed not only larger pre-associates (slow modes), but also very small object (fast modes) with radii ca. 2 – 3 nm that can be attributed to single chains that can be both free or decorated by  $[\text{CoD}]^-$  clusters. At certain  $\xi$ , the slow modes have been no longer detected for both samples by DLS. They could disappear or their light scattering contribution to the overall signal is too low to be detected.

## Additional cryoTEM characterization of nanoparticles

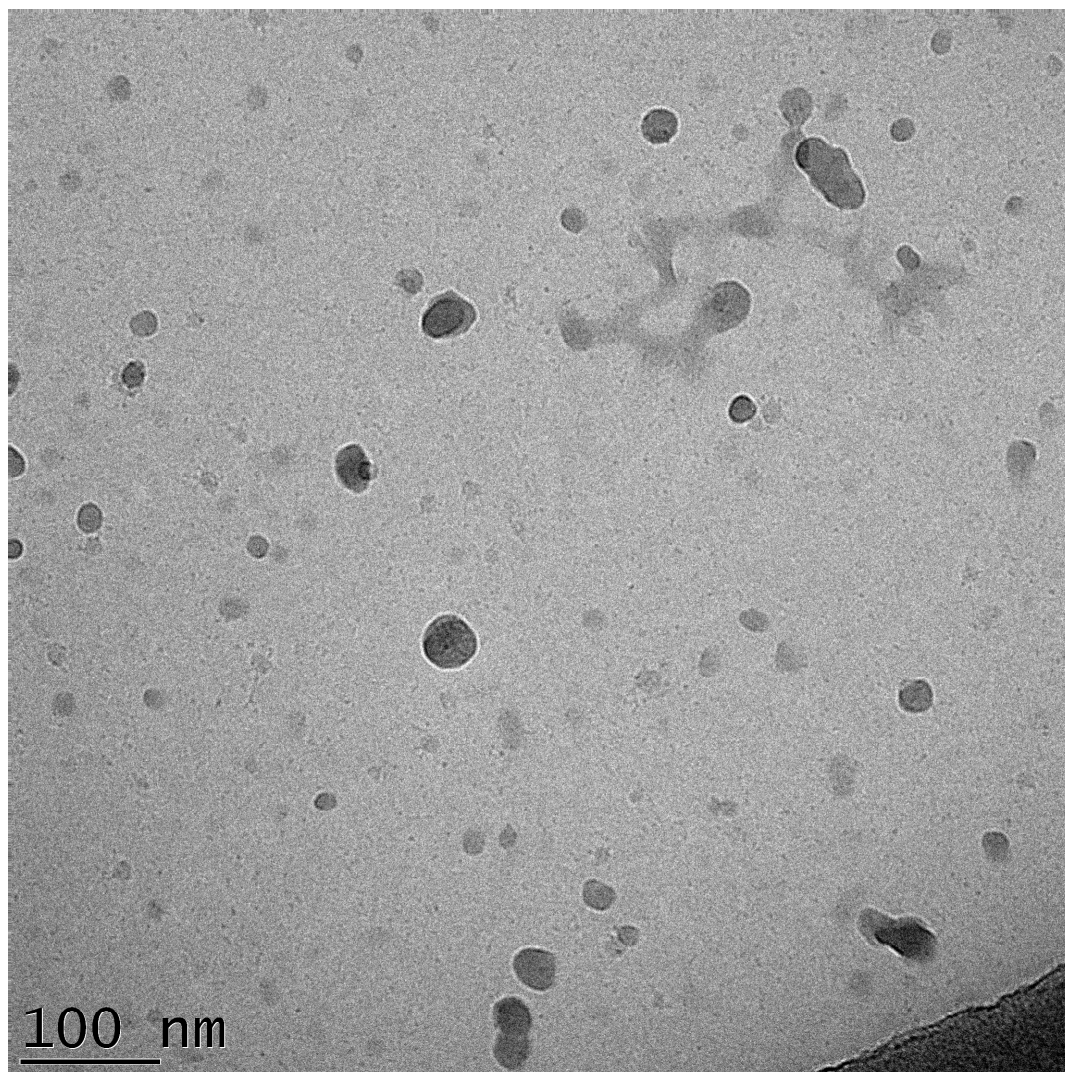


**Figure S5** Typical cryo-TEM micrographs of triblock PEOX-PEO-PEOX/Na[CoD] in 0.154 M NaCl, ( $\xi = 0.4$ ). Even though the nanoparticles are not such regular as in the case of PEO-PEOX/Na[CoD], they are also homogeneous with no sign of compartmentalization.

## ITC characterization of nanoparticles

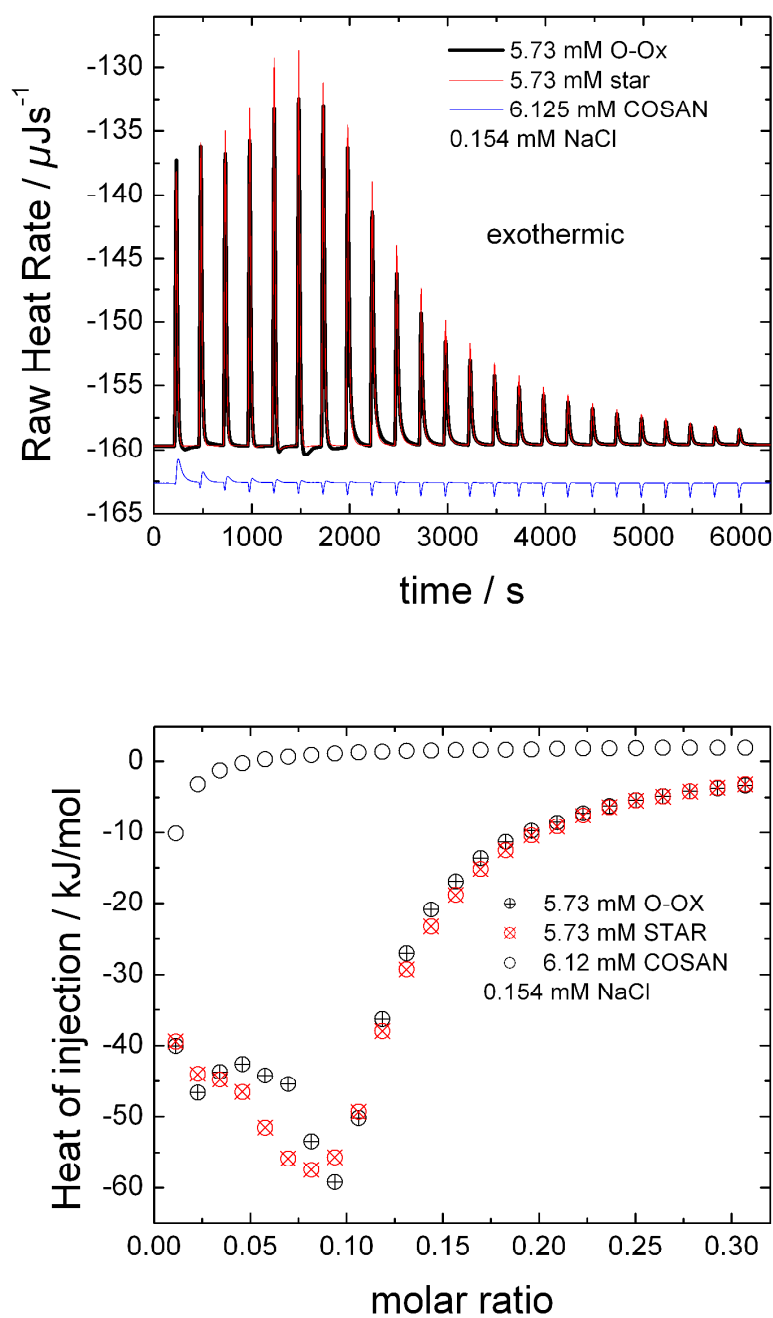


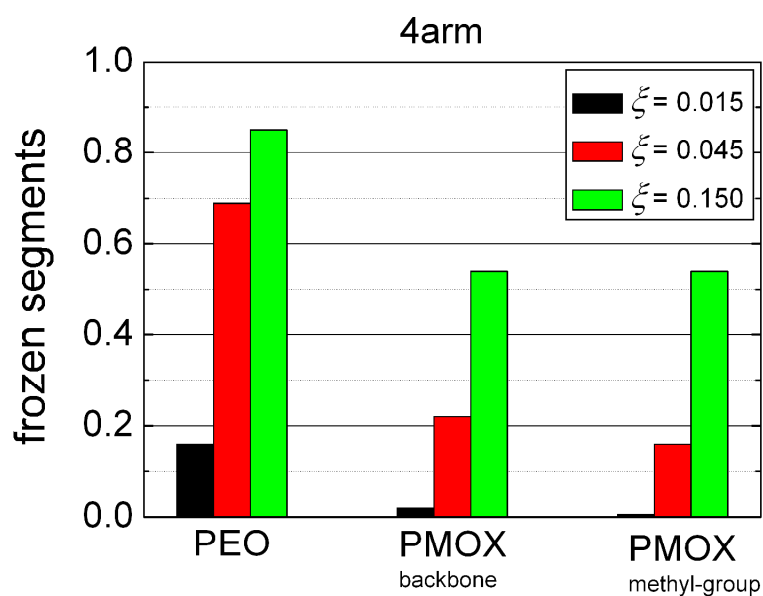
**Figure S6** (A) Raw ITC response for 6.125 mM Na[CoD] titrated into (red) [PEO-PMOX]<sub>4</sub>, (black) PEO-PEOX and (blue) blank solution in 0.154 M NaCl. (B) ITC thermograms for 6.125 mM Na[CoD] titrated into (red) [PEO-PMOX]<sub>4</sub>, (black) PEO-PEOX and (hollow spheres) blank solution in 0.154 M NaCl.

Additional information can be obtained from ITC curves (Figure S6B). A slight difference is apparent from the fact that the “peak” at approximately 0.1 is sharper for the linear diblock than in the case of the 4-arm copolymer, resembling the so-called “aggregation peak” previously observed for PEO homopolymers (Figure S3A).<sup>4,5</sup> This result is consistent with the scenario in which hybrid nanospheres are created by the sudden attraction of originally loose, mobile and randomly intermixed polymeric segments of linear diblock. The formation of [PEO-PMOX]<sub>4</sub>/Na[CoD] nanoparticles is rather based on the consecutive addition of smaller building blocks, accompanied by an increase of their compactness; no thorough reorganization is necessary.

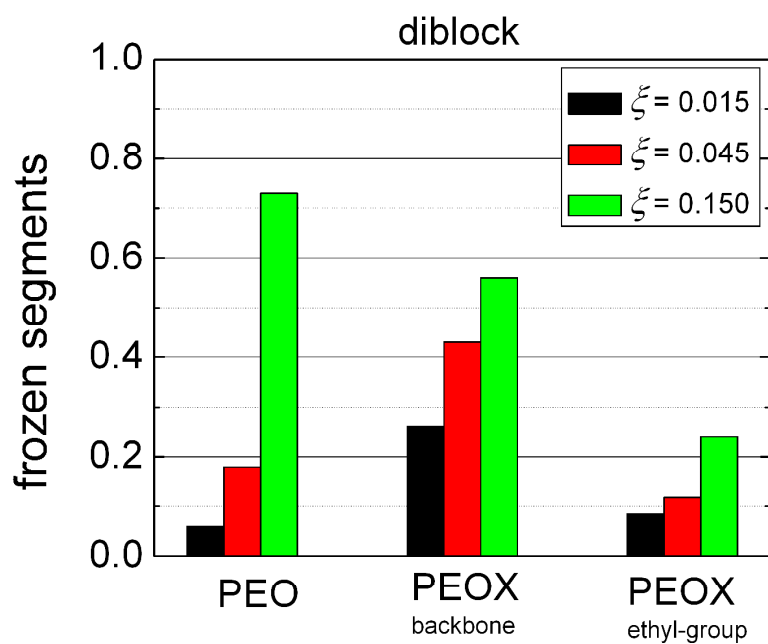
## NMR characterization of nanoparticles

The fraction of frozen segments has been calculated from a diminishing of  $^1\text{H}$  NMR signal of corresponding units after addition of  $\text{Na}[\text{CoD}]$ . We took advantage from the well-known fact that the NMR signal decreases and the spectrum is broadened, if the mobility of corresponding moiety is restricted due to the formation of complex with metallocaborane. We added certain amount of an internal standard (t-butanol) to solutions of pure copolymers (see spectra in Fig.S1) and to their mixtures with  $\text{Na}[\text{CoD}]$ . After that we compared ratios of all the copolymers signals to tBuOH signal (1.25 ppm) in solutions with and without  $\text{Na}[\text{CoD}]$ . From the obtained ratios we calculated fraction of “frozen segments”, which are equal to number of segments involved in complexation with metallocaboranes. Further comments could be found in Refs.5.

The following signals have been examined in  $^1\text{H}$  NMR spectra of PEO-PEOX and [PEO-PMOX]<sub>4</sub>: ethylene moieties in PEO (3.7 ppm) and POX backbones (3.65 – 3.4 ppm); methylene (2.4 ppm) and methyl (1.1 ppm) moieties of ethyl side group in PEOX; methyl side group (2.1 ppm) in PMOX. In general, we found that the mobility of backbone is the most restricted as compared to side groups. Both signals from ethyl side-group are almost equally restricted (the numbers shown in the graph are averages from both signals).



A



B

**Figure S7** Fraction of frozen polymeric segments in (A) [PEO-PMOX]<sub>4</sub>/Na[CoD] and (B) PEO-PEOX/Na[CoD] (right) differing in Na[CoD] content in 0.154 M NaCl calculated from a decrease of corresponding <sup>1</sup>H NMR signals related to pure PEO-PEOX and *t*-butanol (internal standard).

## AFM imaging of nanoparticles

Samples for AFM were prepared by dip coating of very dilute (around 0.01 g/L) nanoparticle aqueous dispersions on freshly cleaved mica surface followed by evaporation of water in vacuum oven. [PEO-PMOX]<sub>4</sub>/Na[CoD], PEO-PEOX/Na[CoD] and PEO-PEO-PEOX/Na[CoD] nanoparticles are visualized by AFM in tapping mode (Figures S3-A -B, and -C respectively). They are of a round shape with no evidence of compartmentalization for [PEO-PMOX]<sub>4</sub>/Na[CoD] (in topology as well as in phase image) due to a broadening effect of AFM probe, a similar stiffness of PEO/Na[CoD] and POX/Na[CoD] domains and mainly the fact that the size of compartments revealed by other methods (cryoTEM and SAXS) is far below the AFM resolution. However, the section analysis of the nanoparticles (Figure S3-C) reveals that [PEO-PMOX]<sub>4</sub>/Na[CoD] nanoparticles adopt a more pronounced pancake shape on the mica surface as compared to both PEO-PEOX/Na[CoD] and PEO-PEO-PEOX/Na[CoD] nanoparticles, which are more round and compact.

We know from our previous research<sup>6</sup> that the size distribution of micelles in solution is strongly correlated with that one on a mica surface after the solvent evaporation. The shape of nanoparticles visualized by AFM is considerably deformed due to the broadening effect of AFM probe and drying on the mica surface. We assume that the extent of deformation is substantially influenced by the particle morphology and density. We therefore assume that homogeneous nanoparticles without compartmentalization suffer from a deformation on mica surface to a lesser extent than those with small compartments glued together by loose POX/Na[CoD] segments. It indicates that PEO-PEOX/Na[CoD] forms homogeneous nanoparticles, while [PEO-PMOX]<sub>4</sub>/Na[CoD] nanostructures are more loose and compartmentalized.

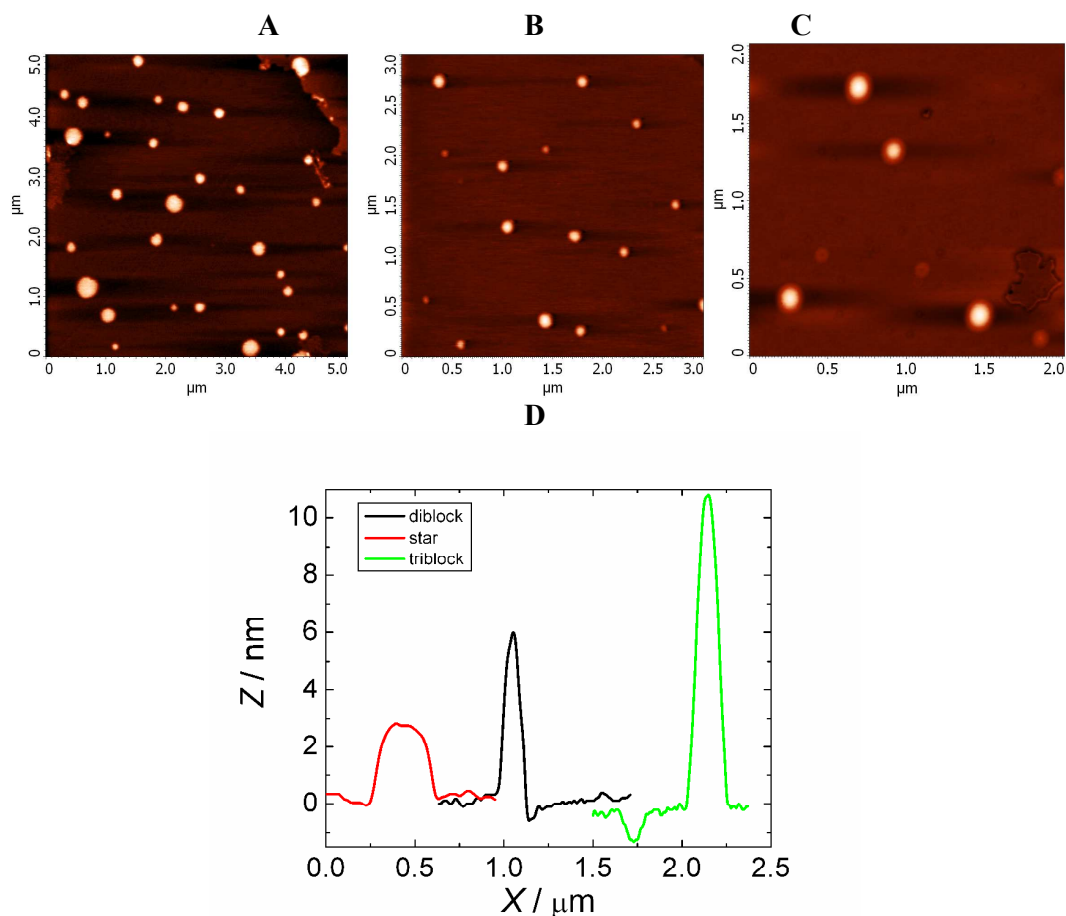


**Figure S8** Typical AFM scans of (A) star [PEO-PMOX]<sub>4</sub>/Na[CoD], (B) diblock PEO-PEOX/Na[CoD], and (C) triblock PEOX-PEO-PEOX/Na[CoD] nanoparticles in 0.154 M NaCl ( $\xi = \text{ca. } 0.2$ ) deposited on a flat mica surface. (D) Cross-sectional analysis of micelles in (A), (B) and (C).

## SAXS and SANS characterization of nanoparticles

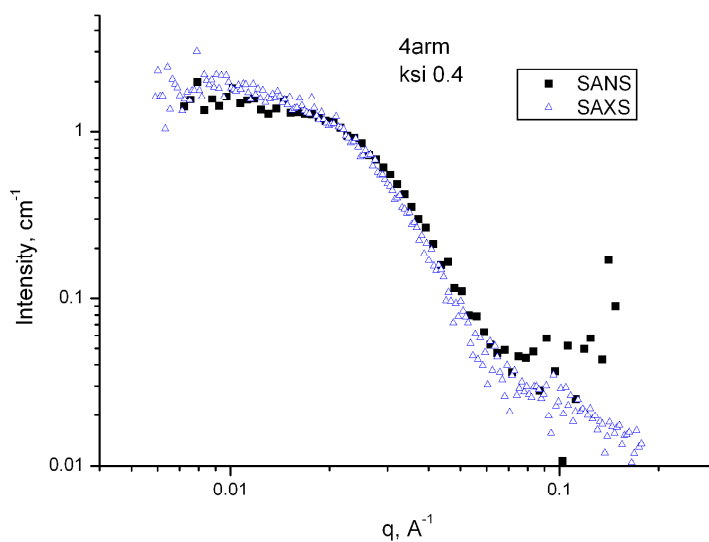


**Figure S9** Comparison of SAXS and SANS curves for [PEO-PMOX]<sub>4</sub>/Na[CoD] with concentration of polymer ca. 2 g/L and  $\xi = 0.4$  in 0.154 M NaCl

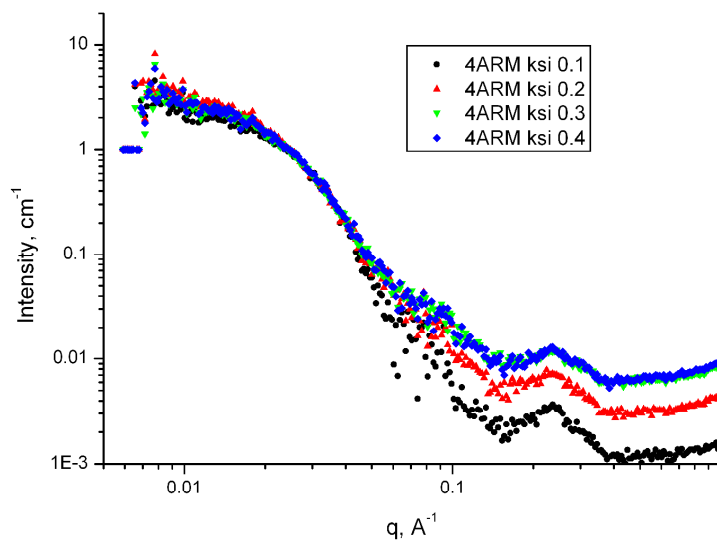


**Figure S10** SAXS curves for [PEO-PMOX]<sub>4</sub>/Na[CoD] in 0.154 M NaCl with concentration of polymer ca. 10 g/L and  $\xi$  in the range 0.1 – 0.4.

**Table S2** The whole SAXS curve could be described with the form factor of sphere with Schultz-Zimm distribution of radius

Sample	Radius, A	Shultz-Zimm Distribution	Extrapolated Intensity, $\text{cm}^{-1}$	Polymer concentration, g/L	Na[CoD] Concentration, g/L	$I/c$
4arm0.1	76.613	0.144	2.94	9.37	5.44	5.04
4arm0.2	71.17	0.236	4.34	8.81	10.23	4.39
4arm0.3	71.586	0.2	3.5	8.32	14.48	6.51
4arm0.4	69.7	0.214	3.62	7.87	18.28	7.22

**Determination of aggregation number,  $N^{\text{agg}}$ , for [PEO-PMOX]<sub>4</sub>/Na[CoD],  $\xi = 0.1$**

1.  $c(\text{[PEO-PMOX]}_4) = 9.37 \text{ g/L}$ ;  $c(\text{Na[CoD]}) = 5.44 \text{ g/L}$ ; Total concentration =  $9.37 + 5.44 = 14.81 \text{ g/L}$

2. Assuming 80 Na[CoD] per 1 polymer chain (from ITC data; Figure S6B):

$$M_w(\text{[PEO-PMOX]}_4) = (3700 + 5600) \cdot 4 = 37200 \text{ g/mol}$$

$$M(\text{Na[CoD]}) = 80 \cdot 346.74 = 27739 \text{ g/mol}$$

$$\text{Total } M_w(\text{chain}) = 64939 \text{ g/mol}$$

3. Equation for  $M_w$  determination from SAXS:  $M_w = \frac{I_0}{c} \cdot \frac{N_a}{\Delta b^2}$ , where  $N_a$  – Avogadro's number ( $6.0221415 \times 10^{23}$ ) and  $\Delta b^2$  – scattering contrast ( $\Delta b^2 = 0.606 \times 10^{23}$  considering density of [PEO-PMOX]<sub>4</sub>/Na[CoD] to be  $\sim 1.185 \text{ g/cm}^3$ ) (ATTENTION! This method is very sensitive to the density value!)

4. For the given sample  $\frac{I_0}{c} = 177.58$ :

$$\text{Experimental } M_w(\text{exp}) \text{ of the particle} = 1764664 \text{ g/mol}$$

$$N^{\text{agg}} = M_w(\text{exp})/M_w(\text{chain}) = 30$$

$\Delta b = b - \bar{V}\rho$ , where  $b[\text{cm/g}]$  is the scattering length (Scattering amplitude) of the dissolved compound,  $\rho [\text{cm}^{-2}]$  is the scattering length density of the solvent,  $\bar{V} [\text{cm}^3/\text{g}]$  is the partial specific volumes (partial specific volume is an inverse of density of dissolved compound).

**Table S3** Characterization of correlation peak (LogNormal) in SAXS curves

Sample	peak position	width	Area	Shape
4arm0.1	0.230475	0.11472	0.000252	1.19913
4arm0.2	0.227245	0.138881	0.000589	1.09466
4arm0.3	0.232401	0.11823	0.000622	1.08613
4arm0.4	0.236553	0.124628	0.000691	0.961982

The peak area is increasing, indicating the increased amount of interacted compartments. This is confirmed by increasing  $I/c$  (Table S2), which is related to the molecular weight of the

particle. Leveling off the peak area vs.  $\xi$  indicates saturation of nanoparticles by metallacarborane at  $\xi \geq 0.2$  (Figure S11), which is consistent with ITC data (Figure S7). It means that a certain part of Na[CoD] is located outside the nanoparticles and it cannot provide trustworthy calculations for such samples.

A peak corresponding to the dimensions of  $[\text{CoD}]^-$  ( $6 \times 11 \text{ \AA}$ ) has not been detected, thus precluding the direct contact of  $[\text{CoD}]^-$  clusters in hybrid nanoparticles.

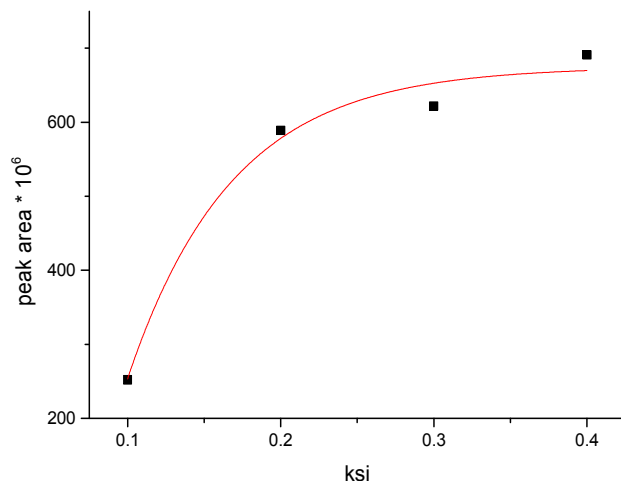


**Figure S11** Dependence of the area of correlation peak in SAXS curves for [PEO-PMOX]<sub>4</sub>/Na[CoD] in 0.154 M NaCl with concentration of polymer ca. 10 g/L on  $\xi$ .

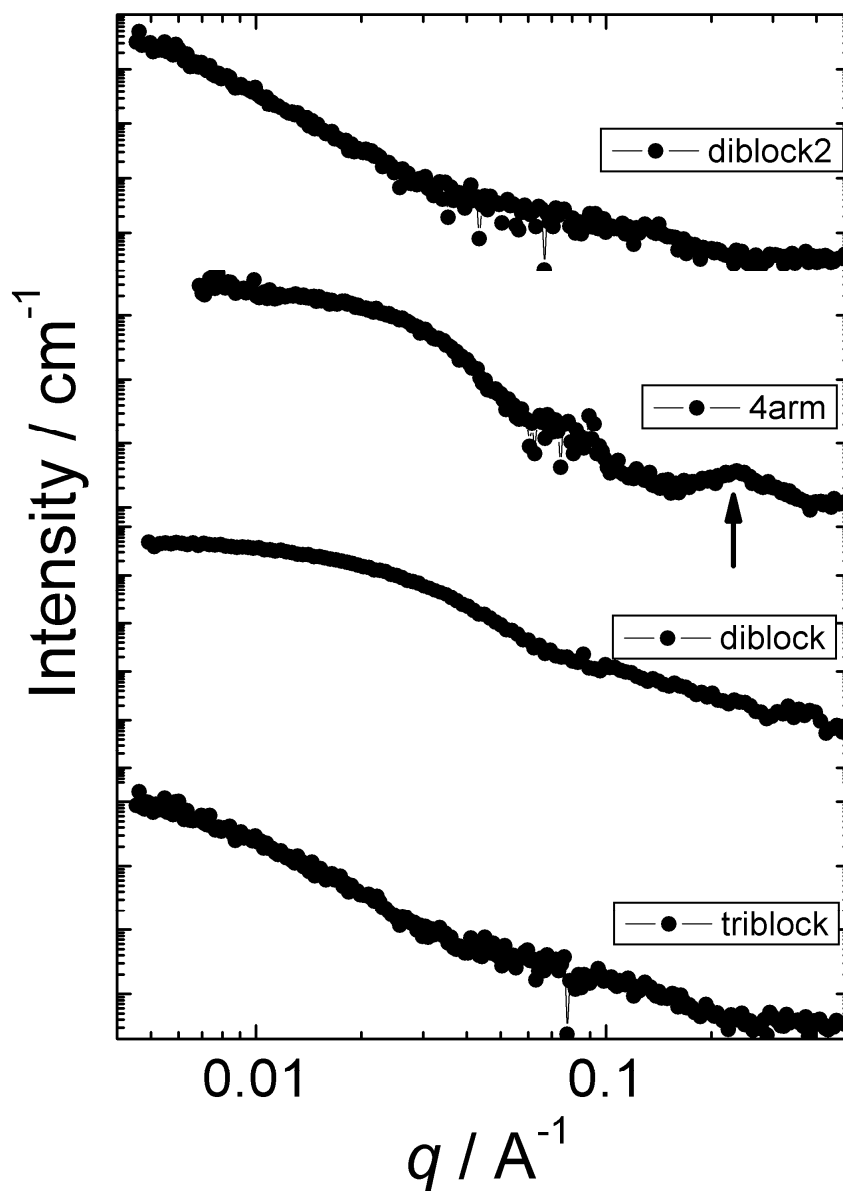


**Figure S12** Comparison of SAXS curves for (diblock2) PEO-PEOX(2)/Na[CoD], (4arm) [PEO-PMOX]<sub>4</sub>/Na[CoD], (diblock) PEO-PEOX/Na[CoD], and (triblock) PEOX-PEO-PEOX/Na[CoD] nanoparticles in 0.154 M NaCl with  $c$  ca. 10 g/L and  $\xi$  ca. 0.1. Only 4arm nanoparticles exhibit correlation peak assigned to compartments (indicated by arrow); all samples of linear copolymers have not any inner organized structure.

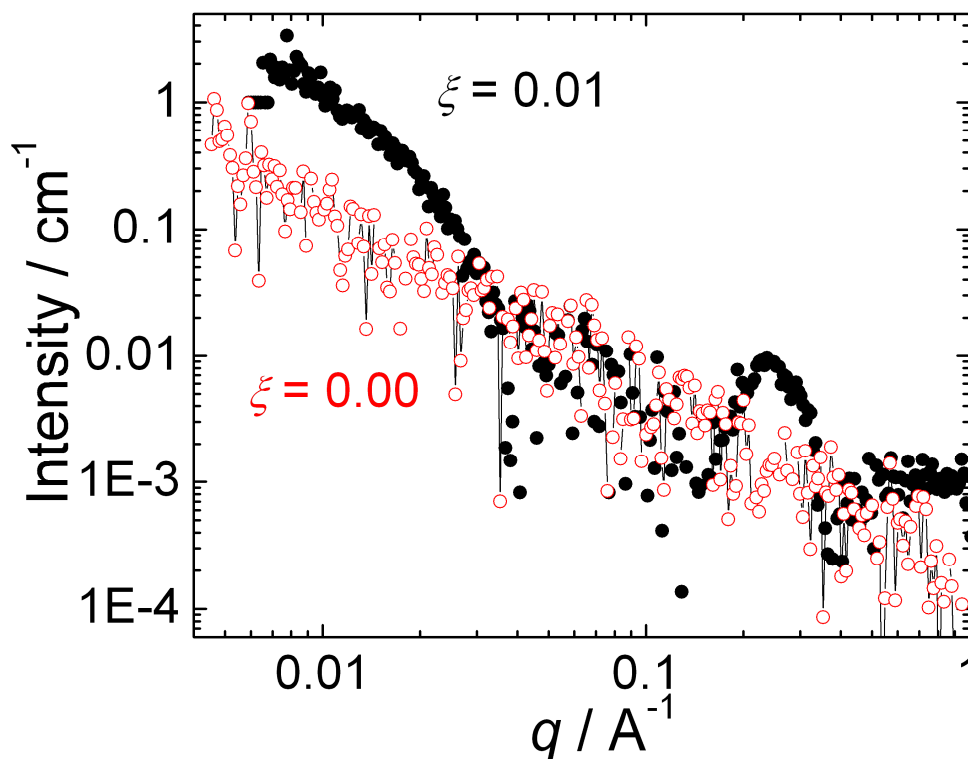


**Figure S13** SAXS curves for pure star-like copolymer [PEO-PMOX]<sub>4</sub> and [PEO-PMOX]<sub>4</sub>/Na[CoD] with very low  $\xi$  (0.01) in 0.154 M NaCl with concentration of polymer ca. 10 g/L. While pure copolymer is molecularly dissolved, appearance of correlation peak at  $q = 0.23 \text{ \AA}^{-1}$  indicates that the PEO/Na[CoD] compartments form even at very low Na[CoD] content (compare with NMR data in Figure S7A).

## References:

- (1) Plesek, J.; Base, K.; Mares, F.; Hanousek, F.; Stibr, B.; Hermanek, S. *Collect. Czech. Chem. Commun.* **1984**, *49*, 2776.
- (2) Kuklin, A. I.; Islamov, A. Kh.; Gordeliy *Neutron News* **2005**, *16(3)*, 16-18.
- (3) Solov'ev A G, Solov'eva T M, Stadnik A V, et al., Report JINR, R10-86, 2003.
- (4) Matejcek, P.; Brus, J.; Jigounov, A.; Plestil, J.; Uchman, M.; Prochazka, K.; Gradzielski, M. *Macromolecules* **2011**, *44*, 3847.
- (5) Dordovic, V.; Uchman, M.; Prochazka, K.; Zhigunov, A.; Plestil, J.; Nykanen, A.; Ruokolainen, J.; Matejcek, P. *Macromolecules* **2013**, *46*, 6881.
- (6) Matejcek, P.; Stepanek, M.; Uchman, M.; Prochazka, K.; Spirikova, M. *Collect. Czech. Chem. Commun.* **2006**, *71*, 723.